

# Inhibition of miR-9 decreases osteosarcoma cell proliferation

Wu Gang<sup>1#</sup>, Wei Tanjun<sup>1#</sup>, Huang Yong<sup>2</sup>, Qin Jiajun<sup>1</sup>, Zhang Yi<sup>3</sup>, Hu Hao<sup>1,2\*</sup>

## ABSTRACT

Osteosarcoma (OS) is the most common primary bone tumor that affects adolescents and young adults. Disruption of microRNA (miRNA) regulation is well established in the pathophysiology of different cancers, including OS. Increased expression of miR-9 in OS positively correlates with the tumor size, clinical stage, and distant metastasis. In the present study, we used two different OS cell lines, MG-63 and Saos-2, as *in vitro* models. miR-9 inhibitor and miR-9 mimics were used to study the function of miR-9 in these two cell lines. We determined the effect of miR-9 inhibition on cell proliferation, cell cycle, apoptosis, and the protein expression of different genes. Our results demonstrated that miR-9 inhibition in the human OS cell lines suppresses their metastatic potential, as determined by decreased cell proliferation and cell cycle arrest, decreased invasion, and increased apoptosis. The Western blot analysis showed that E-cadherin, matrix metalloproteinase 13, forkhead box O3, Bcl-2-like protein 11, and  $\beta$ -catenin are involved in miR-9 signaling. Moreover, miR-9 mimics rescued the effects caused by the inhibition of miR-9 in the OS cell lines. Our findings suggest that miR-9 is important for mediating OS cell migration, invasion, metastasis, and apoptosis. Inhibition of miR-9 could be further explored as a therapeutic target to treat OS.

KEYWORDS: Osteosarcoma; cell proliferation; metastasis; miR-9; E-cadherin; CDH1; matrix metalloproteinase 13; MMP-13; forkhead box O3; FOXO3a; Bcl-2-like protein 11; BCL2L11;  $\beta$ -catenin; CTNNB1

## INTRODUCTION

Osteosarcoma (OS) is the most common primary bone tumor that affects adolescents and young adults. Because these tumors have a high metastasis capability, they are considered as the most frequent cause of cancer-related morbidity and mortality. Surgery and chemotherapy are the standard approaches for the treatment of the disease. Although the prognosis of OS has improved with these standard regimens, the overall survival remains unsatisfactory due to a high metastasis rate [1-3]. Despite various efforts of the research community, the mechanism underlying OS development remains unclear.

MicroRNAs (miRNAs) are small non-coding, regulatory RNAs that play critical roles in various cellular processes such as

cell proliferation, growth, and chemosensitivity [2,4,5]. Although miRNAs are small in size (ranging between 18 and 25 nucleotides in length), they recognize and bind specific target mRNAs by complete or partial base pairing mostly at the 3'-untranslated region (UTR) of the target genes to post-transcriptionally regulate gene expression. Since their discovery, more than 1000 miRNAs have been identified, which possibly regulate 50% of human genes and thousands of gene transcripts [2,6,7].

Previously, using a bioinformatics approach, we demonstrated differential expression of several miRNAs in OS and osteoblast cell lines [8]. The expression of miR-9, miR-99, miR-195, miR-148a, and miR-181a was found to be significantly increased in MG-63 OS cell line compared with osteoblasts. These results were further validated using quantitative reverse transcription PCR (qRT-PCR) [8]. On the contrary, miR-143, miR-145, miR-335, and miR-539 were found to be downregulated in OS cells [8]. Xu et al. demonstrated a significantly increased expression of miR-9 in OS tissue compared to healthy bone tissue [9]. The increased expression of miR-9 in OS positively correlated with the tumor size, clinical stage, and distant metastasis [9]. These results suggest an important role of miR-9 in the regulation of OS progression. The abnormal expression of miR-9 has been demonstrated in other cancers, including ovarian cancer [10], renal cell carcinoma [11], gastric cancer [12], and colon cancer [13]. miR-9 was shown to participate in metastasis by regulating its target genes, including E-cadherin (*CDH1*), glycogen synthase kinase 3 beta (*GSK3 $\beta$* ), Bcl-2-like protein 11 (*BCL2L11*), and matrix metalloproteinases (MMPs) [12,14,15].

<sup>1</sup>Department of Orthopedics, Central Theater Command General Hospital of the Chinese People's Liberation Army, Wuhan, Hubei, China

<sup>2</sup>Department of Orthopedics, Hubei Provincial Hospital of Traditional Chinese Medicine, Wuhan, Hubei, China

<sup>3</sup>Department of Orthopedics, The First Affiliated Hospital of Zhengzhou University, Zhengzhou, Henan, China

\*Corresponding author: Hu Hao, Department of Orthopedics, Central Theater Command General Hospital of the Chinese People's Liberation Army, No. 627 Wuluo Road, Wuhan, Hubei, China. Phone: 86-27-50772528. E-mail: 12914219@qq.com

<sup>#</sup>These authors equally contributed

DOI: <https://dx.doi.org/10.17305/bjbms.2019.4434>

Submitted: 01 September 2019/Accepted: 12 November 2019

Conflict of interest statement: The authors declare no conflict of interests



©The Author(s) (2020). This work is licensed under a Creative Commons Attribution 4.0 International License

In the present study, we demonstrated that miR-9 inhibition in human OS cell lines suppressed their metastatic potential as determined by decreased invasion and increased apoptosis. Furthermore, we showed that proteins such as E-cadherin, MMP-13, forkhead box O3 (FOXO3a), Bcl2-L-11, and  $\beta$ -catenin are involved in the miR-9 signaling and could be further explored as therapeutic targets to treat OS.

## MATERIALS AND METHODS

### Antibodies

The following antibodies against human proteins were used: E-cadherin (Abcam, MA, USA; ab40772, 1:20000),  $\beta$ -catenin (Abcam, MA, USA; ab32572, 1:8000), MMP-13 (Abcam, MA, USA; ab39012, 1:4000), Bcl2-L-11 (Abcam, MA, USA; ab32158, 1:500), FOXO3a (Abcam, MA, USA; Ab47409, 1:800), GSK3 $\beta$  (Proteintech Group Inc., IL, USA; 22104-1-AP, 1:2000), c-Myc (ProteinTech Group Inc., IL, USA; 10828-1-AP, 1:2000), CD44v6 (ProteinTech Group Inc., IL, USA; 15675-1-AP, 1:2000), vascular endothelial growth factor A [VEGF-A] (ProteinTech Group Inc., IL, USA; 19003-1-AP, 1:1000), cyclin D1 (CST, MA, USA; 2978, 1:1000), B-cell lymphoma 2 [Bcl2] (CST, MA, USA; 2870S, 1:1000), and  $\beta$ -actin (Boster, Wuhan, China; BMO627, 1:200). Secondary antibodies were horseradish peroxidase (HRP)-conjugated goat anti-mouse immunoglobulin (Ig)G (H + L) (Boster, Wuhan, China; BA1051, 1:50000) and goat anti-rabbit IgG (H + L) (Boster, Wuhan, China; BA1054, 1:50000).

### Cell culture

OS cell lines MG-63 and Saos-2 were obtained from Type Culture Collection of Chinese Academy of Sciences (Shanghai, China). Cells were maintained in Dulbecco's Modified Eagle Medium [DMEM] (Hyclone, USA) supplemented with 10% fetal bovine serum (Gibco, USA), 50 U/mL penicillin, and 50 mg/mL streptomycin. Exponentially growing cultures were maintained in a humidified atmosphere of 5% carbon dioxide at 37°C.

### Oligonucleotide construction and cell transfection

Inhibitor of miR-9 (5'-UCAUACAGCUAGAUAAACCAAGA-3') and negative control oligonucleotides (miR-NC) (5'-CAGUACUUUUGUGUAGUACAA-3') were chemically synthesized and were ready for use (GenePharma Co. Ltd., Shanghai, China). Untreated cells served as a control in all experiments. A working 20  $\mu$ M stock solution was prepared in sterilized ddH<sub>2</sub>O and stored at -80°C. For transfection, the optimal concentration for both cell lines was 100 nM. In brief, the cells ( $1 \times 10^6$ ) were seeded in a 6-well plate and incubated with complete medium overnight, to obtain a confluence of 40–50%. The next day, cells were transiently transfected with either miR-9 inhibitor

or NC oligonucleotides ( $5 \times 10^5$  cells) with Lipofectamine 2000 (Invitrogen, CA, USA) as per the manufacturer's instructions. miR-9 mimics (UCUUUGGUUUAU CUAGCUGUAUGAAUACA GCUAGAUAAACC CAAAGAUU) were purchased from GenePharma Co. Ltd., Shanghai, China. In the experiments where both miR-9 mimics and inhibitor were used, cells were treated with miR-9 inhibitor first and then with the mimics at a concentration of 100 nM.

### RNA extraction and qRT-PCR

Total RNA was extracted from cells using miRNeasy Mini Kit (QIAGEN, Germany), according to the manufacturer's instructions. RNA concentration and quality were measured using the spectrophotometer (ND-2000, NanoDrop, DE, USA). To detect the expression of miR-9, qRT-PCR was performed using the Bulge-Loop™ miRNA qRT-PCR Primer Set (Ribobio, Guangzhou, China). Primers for miR-9 and U6 were purchased from Ribobio, Guangzhou, China. All quantitative PCR reactions, including no-template controls, were performed in triplicate. Expression levels of miRNAs were evaluated using the comparative threshold cycle (Ct) method as normalized to that of U6.

### Cell proliferation assay

MG-63 and Saos-2 cells transfected with miR-9 inhibitor or respective NC were plated in triplicate in a 96-well plate ( $2 \times 10^3$  cells). Cell proliferation was measured at different time points using the Click-iT EdU kit (KGA331-50, KeyGEN BioTECH, Nanjing, China), according to the manufacturer's instructions.

### Cell apoptosis assay

Cell apoptosis was detected using the Annexin V-APC/7AAD apoptosis detection kit (KGA108, KeyGEN BioTECH, Nanjing, China). In brief,  $1 \times 10^5$  untreated or treated cells were harvested following trypsinization and centrifugation, after transfection at different time points. Cells were washed with phosphate-buffered saline (PBS) and resuspended in 500  $\mu$ L binding buffer, to which 5  $\mu$ L 7-AAD was added; after 10 min incubation, 1  $\mu$ L Annexin V-APC was added followed by 10 min incubation in the dark. Apoptotic cells were analyzed by flow cytometry (FACSCalibur, BD Biosciences, USA).

### Cell cycle assay

Flow cytometry assay was used to determine the cell cycle distribution (KGA512, KeyGEN BioTECH, Nanjing, China) as described previously [16].

## Cell invasion assay

Cell invasion assay was performed as described previously [17]. Briefly, the membranes of the modified chambers containing Transwell polycarbonate membranes (Costar, Cambridge, MA, USA) were coated with 100 µg/mL Matrigel (Sigma),  $1 \times 10^5$  cells were seeded into the upper chamber. After 48 h incubation, cells that invaded the Matrigel and polycarbonate membrane to the lower surface were stained with 0.2% crystal violet. The data are presented as the average number of cells attached to the bottom surface from five randomly chosen fields.

## Western blotting

Cell lysates were prepared in cell lysis buffer with protease cocktail inhibitor (Thermo Fisher Scientific, Waltham, MA, USA). Cellular debris was cleared from lysates by centrifugation, and protein concentrations were determined using an enhanced Bicinchoninic Acid (BCA) Protein Assay Kit (P0010, Beyotime Co., China). Approximately 20 µg of protein per lane were separated using sodium dodecyl sulfate-polyacrylamide gel electrophoresis (SDS-PAGE) and transferred to the membrane, and proteins were visualized using enhanced chemiluminescence [ECL] (ECL Detection System; Amersham Pharmacia Biotech, UK). Quantification of Western blots was performed using ImageJ v.64 software (National Institutes of Health, Bethesda, MD, USA). Protein levels were calculated by normalizing the band intensities of the test protein to that of the loading control (actin) and presented as arbitrary units.

## Statistical analysis

All data are expressed as mean  $\pm$  standard deviation (SD). Statistical analysis was done using SPSS Statistics for Windows, Version 17.0. (SPSS Inc., Chicago, IL, USA). Results were considered statistically significant only if  $p < 0.05$ . Each experiment was run a minimum of three times.

## RESULTS

MG-63 and Saos-2 OS cell lines, used in the present study, overexpress miR-9 [8]. Using a specific miR-9 inhibitor, the expression of miR-9 was significantly downregulated in both OS cell lines compared to controls (Figure 1A). Next, we determined the effect of miR-9 inhibitor on cell proliferation. We observed that the inhibition of miR-9 significantly reduced cellular proliferation in both OS cell lines compared to controls, as determined by the fluorescent-based Click-iT EdU kit (Figure 1B and C).

Reduction in cell proliferation with an increased rate of apoptosis is well described in different cancer cells [18]. We

next measured the rate of apoptosis in OS cells in the presence of miR-9 inhibitor. MG-63 cells transfected with miR-9 inhibitor for 48 h showed an increase in apoptosis rate compared to NC group (Figure 1D and E). Increased apoptotic cell populations were also observed among miR-9 inhibitor-transfected cells, with  $\sim 2.5$ -fold and  $\sim 2.6$ -fold increases in apoptotic cell numbers in MG-63 and Saos-2 cells, respectively compared to miR-NC-transfected cells (Figure 1D and E). Cell cycle analysis showed that the inhibition of miR-9 increased the number of cells in the subG1 population in both MG-63 and Saos-2 cell lines compared to respective controls (Figure 1F-H). These results suggest that inhibition of miR-9 exerts tumor-suppressive effects by inducing cell cycle arrest in G1 phase and increasing apoptosis.

Transwell invasion assay was performed to evaluate the role of miR-9 in OS metastasis. We observed that the percentage of invaded cells through Transwell membrane significantly decreased after miR-9 inhibition compared to respective controls (Figure 2).

To get further insight into the mechanism and considering the role of miR-9 in metastasis of different cancers, we explored the effect of miR-9 inhibition on the expression of E-cadherin, GSK3 $\beta$ , Bcl2-L-11, and MMP-13 [12,14,15]. Our results showed that the inhibition of miR-9 increased the protein expression of E-cadherin, GSK3 $\beta$ , Bcl2-L-11, MMP-13, and FOXO3a and decreased the expression of  $\beta$ -catenin, c-Myc, cyclin D, Bcl2, VEGF-A, and CD44v6 in OS cells (Figure 3A and B).

Further, to confirm the effects of miR-9 on OS cells, we performed rescue experiments using miR-9 mimics. The transfection with miR-9 mimics significantly increased the expression of miR-9 in both cell lines as determined by qRT-PCR (Figure S1A). miR-9 mimics were able to rescue the effects of miR-9 inhibition in different assays as demonstrated in Figure S1B-G. The miR-9 mimic treatment significantly decreased the expression of E-cadherin and GSK3 $\beta$  and increased  $\beta$ -catenin expression in both cell lines. The treatment with miR-9 mimics, however, failed to completely rescue the effects of miR-9 inhibitor in these cells as demonstrated by Western blot analysis (Figure S1H). These results clearly indicate the direct involvement of miR-9 in OS cell proliferation and migration.

## DISCUSSION

Despite recent advances in diagnosis and treatment of osteosarcoma (OS), the mortality rate remains high, suggesting an urgent need to develop a more effective therapy. Dysregulation of miRNAs is well known to play a role in the initiation and progression of human cancer [1]. Clinical and experimental studies using miRNAs have gained much interest to understand the pathogenesis and explore miRNAs as



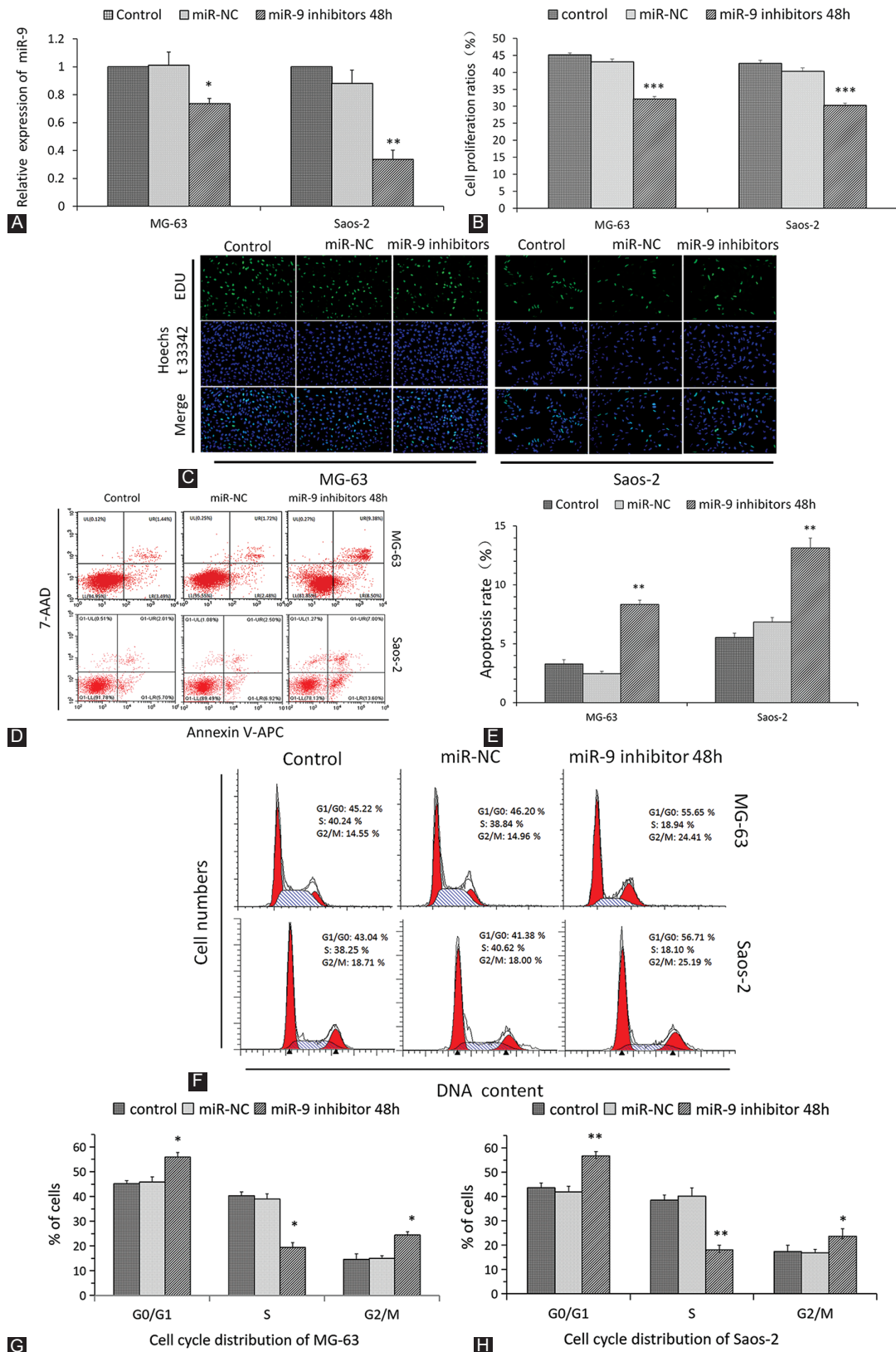


**FIGURE 1.** Effect of miR-9 inhibition on cell proliferation, apoptosis, and cell cycle. (A) miR-9 inhibitor significantly decreased the expression of miR-9 in MG-63 and Saos-2 osteosarcoma (OS) cells as determined by quantitative reverse transcription PCR (qRT-PCR); (B and C) miR-9 inhibition decreased the cell proliferation as determined by fluorescent-based kit. Panel B shows the quantitation of cell proliferation and panel C shows the representative microscopic pictures of OS cells. (D and E) Apoptotic cells, PE (+) and 7-AAD (-), were analyzed using flow cytometry in OS cells. Apoptosis significantly increased with the use of miR-9 inhibitor in OS cell lines. Panel D shows the flow cytometry dot plots and panel E shows the quantitation of apoptosis rate. (F-H) miR-9 regulated the cell cycle of OS cells. Panel F shows the flow cytometry histograms and panels G and H show the quantification data for MG-63 and Saos-2, respectively. Data are presented as averages of triplicate measurements with error bars representing standard deviations. \* $p < 0.05$ , \*\* $p < 0.01$ , and \*\*\* $p < 0.001$ .

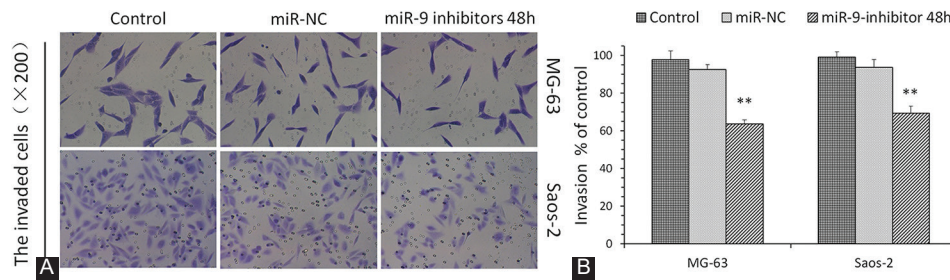


**FIGURE 2.** Effects of miR-9 inhibition on the invasion ability of osteosarcoma (OS) cells. (A) Representative pictures of the invaded OS cells under the membrane, observed under a microscope. Scale bar = 100 mm. (B) Invasion was quantified by counting the number of MG-63 and Saos-2 cells that invaded into the inner membrane. Data are presented as averages of triplicate measurements with error bars representing standard deviations. \*\* $p < 0.01$ .

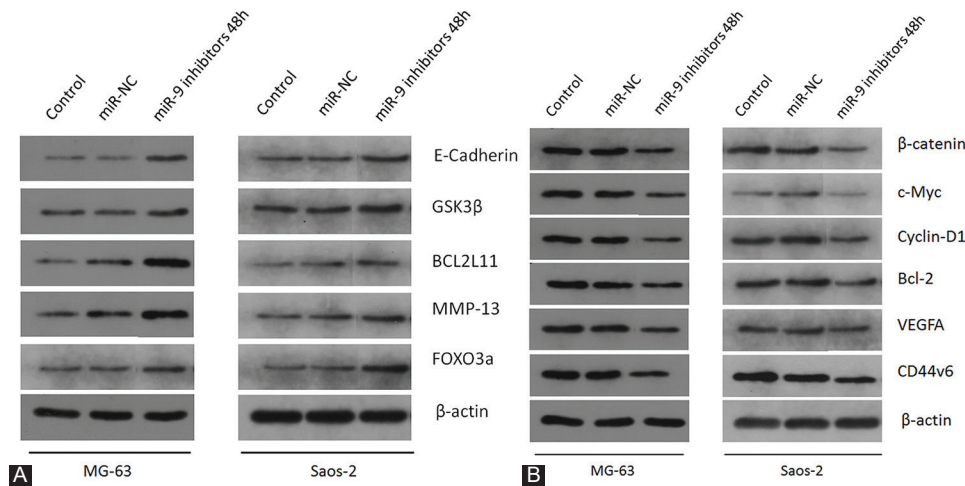


**FIGURE 3.** Effect of miR-9 inhibition on E-cadherin, GSK3β, and β-catenin protein expression. miR-9 inhibition increased (A) and decreased (B) the expression of different proteins. The inhibition of miR-9 increased the protein expression of E-cadherin, GSK3β, Bcl2-L-11, MMP-13, and FOXO3a and decreased the expression of β-catenin, c-Myc, cyclin D, Bcl2, VEGF-A, and CD44v6 in OS cells. Western blot results are for a minimum of three experiments. β-actin was used as the loading control. GSK3β: Glycogen synthase kinase 3 beta; BCL2L11: Bcl-2-like protein 11; MMP-13: Matrix metalloproteinase 13; FOXO3a: Forkhead box O3; Bcl2: B-cell lymphoma 2; VEGFA: Vascular endothelial growth factor A.

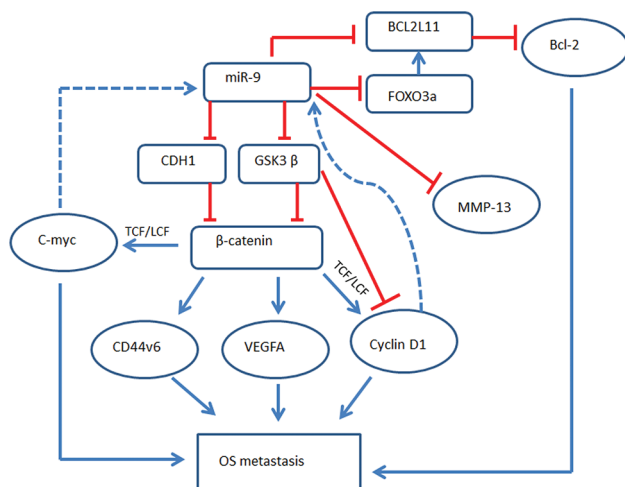


**FIGURE 4.** Potential mechanisms of miR-9 mediated proliferation, apoptosis, and cell cycle regulation in osteosarcoma. Mir-9 inhibits apoptosis (red) and promotes cell proliferation (blue), which ultimately regulates osteosarcoma metastasis. GSK3β: Glycogen synthase kinase 3 beta; BCL2L11: Bcl-2-like protein 11; MMP-13: Matrix metalloproteinase 13; FOXO3a: Forkhead box O3; Bcl2: B-cell lymphoma 2; VEGFA: Vascular endothelial growth factor A; TCF/LCF: T-cell factor/lymphoid enhancer-binding factor.

therapeutic targets [19]. Although miR-9 was first reported as a pro-inflammatory signal regulator [20], recent studies have demonstrated its potential in malignant diseases [21]. Increased expression of miR-9 in OS tissues compared with non-cancerous bone tissues has been observed. Besides, increased miR-9 expression in OS tissues is significantly correlated with clinicopathological features, tumor size, clinical stage, and distant metastasis [2,7,9].

Previously, we demonstrated increased expression of miR-9 in OS cell lines [8]. In the present study, using two different OS cell lines, we showed that the inhibition of miR-9 decreased cell proliferation (Figure 1B and C), increased apoptosis (Figure 1D and E), decreased invasion (Figure 2), and regulated the expression of E-cadherin, GSK3β, and β-catenin (Figure 3). These results suggest that miR-9 exerts oncogenic effects in OS, and are supported by the previous findings [22].

The molecular mechanism of miR-9 effects on metastasis and its target genes are mostly unknown. The validated target genes include nuclear factor kappa B subunit 1 (*NFKB1*), chromodomain helicase DNA binding protein 1 (*CHD1*),

*VEGFA*, vimentin (*VIM*), *MMP13*, and *BCL2* interacting killer (*BIK*) [8]. In a recent study, Gao et al. showed the p16 *CDKN2A* gene to be another target gene of miR-9 in OS [23]. In their study, miR-9 depletion downregulated the extracellular signal-regulated kinase (ERK)/p38/c-Jun N-terminal kinase (JNK) pathway by targeting *CDKN2A* [23].

Abnormal cell cycle causes tumor growth and malignant cell proliferation [16-18]. Liu et al. demonstrated that the inhibition of miR-9 in N2a cells blocks cell cycle in G1 phase [24]. Similarly, we observed that miR-9 inhibitor arrested cell cycle in G1 phase in both OS cell lines (Figure 1F-H).

Further, we analyzed the expression of E-cadherin, cyclin D1, c-Myc, and  $\beta$ -catenin to examine the molecular mechanism underlying miR-9 oncogenic effects in OS cells (Figure 3). Various genetics and epigenetic factors regulate the expression of miRNAs. DNA methylation affects miR-9 expression in colorectal cancer [25], whereas in breast cancer, Myc regulates the expression of miR-9 [26]. A previous study showed that miR-9 targets the E-cadherin *CDH1* gene and leads to scattering and epithelial-mesenchymal transition (EMT)-like conversion of SUM149 cells [26]. Furthermore, Li et al. demonstrated that casein kinase 1 alpha (CK1 $\alpha$ ) and GSK3 $\beta$ , two inhibitors of  $\beta$ -catenin signaling pathway, were direct targets of miR-9-5p in mesenchymal stem cells (MSCs) and that the overexpression of miR-9-5p upregulated  $\beta$ -catenin signaling pathway [27]. Moreover, cellular proliferation and immune escape of tumor cells are generated at any time due to the activation of protooncogenes, such as *FOXO3*, *BCL2L1*, and *GSK3B* [3,12,28]. Based on the results of our and previous studies [2,12,14,15], we propose a model for the action of miR-9 in OS (Figure 4).

Disruption of miRNA regulation plays an important role in the development of cancer. miRNA-based therapies with miRNA mimics and miRNA antagonists can be used to inhibit the expression of genes involved in carcinogenesis and, consequently, to inhibit cancer.

## CONCLUSION

In summary, our findings identify miR-9 as an essential factor for mediating OS cell migration, invasion, metastasis, and potentially apoptosis, and provide relevant evidence for further development of therapeutic method using miR-9.

## ACKNOWLEDGMENTS

This work was supported by Hubei Provincial Natural Science Foundation of China (No. 2016CFB363, No. 2016CFB187) and the funds of Central Theater Command General Hospital (No. YZ201504). We would like to thank Science Pen Group for helping in proofreading the article.

## REFERENCES

- [1] Simpson E, Brown HL. Understanding osteosarcomas. *JAAPA* 2018;31(8):15-9. <https://doi.org/10.1097/01.JAA.0000541477.24116.8d>
- [2] Sampson VB, Yoo S, Kumar A, Vetter NS, Kolb EA. MicroRNAs and potential targets in osteosarcoma: Review. *Front Pediatr* 2015;3:69. <https://doi.org/10.3389/fped.2015.00069>.
- [3] Botter SM, Neri D, Fuchs B. Recent advances in osteosarcoma. *Curr Opin Pharmacol* 2014;16:15-23. <https://doi.org/10.1016/j.coph.2014.02.002>.
- [4] Hesse E, Taipaleenmäki H. MicroRNAs in bone metastasis. *Curr Osteoporos Rep* 2019;17(3):122-8. <https://doi.org/10.1007/s11914-019-00510-4>.
- [5] Kushlinskii NE, Fridman MV, Braga EA. Molecular mechanisms and microRNAs in osteosarcoma pathogenesis. *Biochemistry (Mosc)* 2016;81(4):315-28. <https://doi.org/10.1134/s0006297916040027>.
- [6] Zhang J, Yan YG, Wang C, Zhang SJ, Yu XH, Wang WJ. MicroRNAs in osteosarcoma. *Clin Chim Acta* 2015;444:9-17. <https://doi.org/10.1016/j.cca.2015.01.025>.
- [7] Peng Y, Croce CM. The role of microRNAs in human cancer. *Signal Transduct Target Ther* 2016;1:15004. <https://doi.org/10.1038/sigtrans.2015.4>.
- [8] Hu H, Zhang Y, Cai XH, Huang JF, Cai L. Changes in microRNA expression in the MG-63 osteosarcoma cell line compared with osteoblasts. *Oncol Lett* 2012;4(5):1037-42. <https://doi.org/10.3892/ol.2012.866>.
- [9] Xu SH, Yang YL, Han SM, Wu ZH. MicroRNA-9 expression is a prognostic biomarker in patients with osteosarcoma. *World J Surg Oncol* 2014;12:195. <https://doi.org/10.1186/1477-7819-12-195>.
- [10] Guo LM, Pu Y, Han Z, Liu T, Li YX, Liu M, et al. MicroRNA-9 inhibits ovarian cancer cell growth through regulation of NF-kappaB1. *FEBS J* 2009;276(19):5537-46. <https://doi.org/10.1111/j.1742-4658.2009.07237.x>.
- [11] Hildebrandt MA, Gu J, Lin J, Ye Y, Tan W, Tamboli P, et al. Hsa-miR-9 methylation status is associated with cancer development and metastatic recurrence in patients with clear cell renal cell carcinoma. *Oncogene* 2010;29:5724-8. <https://doi.org/10.1038/onc.2010.305>.
- [12] Zheng L, Qi T, Yang D, Qi M, Li D, Xiang X, et al. MicroRNA-9 suppresses the proliferation, invasion and metastasis of gastric cancer cells through targeting cyclin D1 and Ets1. *PLoS One* 2013;8(1):e55719. <https://doi.org/10.1371/journal.pone.0055719>.
- [13] Cekaite L, Rantala JK, Bruun J, Guriby M, Agesen TH, Danielsen SA, et al. MiR-9, 31, and 182 deregulation promote proliferation and tumor cell survival in colon cancer. *Neoplasia* 2012;14(9):868-79. <https://doi.org/10.1593/neo.121094>.
- [14] Zhou B, Xu H, Xia M, Sun C, Li N, Guo E, et al. Overexpressed miR-9 promotes tumor metastasis via targeting E-cadherin in serous ovarian cancer. *Front Med* 2017;11(2):214-22. <https://doi.org/10.1007/s11684-017-0518-7>.
- [15] Zhang H, Song B, Pan Z. Downregulation of microRNA-9 increases matrix metalloproteinase-13 expression levels and facilitates osteoarthritis onset. *Mol Med Rep* 2018;17:3708-14. <https://doi.org/10.3892/mmr.2017.8340>.
- [16] Zhang Y, Wei RX, Zhu XB, Cai L, Jin W, Hu H. Tanshinone IIA induces apoptosis and inhibits the proliferation, migration, and invasion of the osteosarcoma MG-63 cell line *in vitro*. *Anticancer Drugs* 2012;23(2):212-9. <https://doi.org/10.1097/cad.0b013e32834e5592>.
- [17] Zhang Y, Song L, Cai L, Wei R, Hu H, Jin W. Effects of baicalein on apoptosis, cell cycle arrest, migration and invasion of osteosarcoma cells. *Food Chem Toxicol* 2013;53:325-33. <https://doi.org/10.1016/j.fct.2012.12.019>.
- [18] Mahajan N, Shi HY, Lukas TJ, Zhang M. Tumor-suppressive maspin

- functions as a reactive oxygen species scavenger: Importance of cysteine residues. *J Biol Chem* 2013;288(16):11611-20. <https://doi.org/10.1074/jbc.M112.410852>.
- [19] Sasaki R, Osaki M, Okada F. MicroRNA-based diagnosis and treatment of metastatic human osteosarcoma. *Cancers (Basel)* 2019;11(2):E553. <https://doi.org/10.3390/cancers11040553>.
- [20] Bazzoni F, Rossato M, Fabbri M, Gaudiosi D, Mirolo M, Mori L, et al. Induction and regulatory function of miR-9 in human monocytes and neutrophils exposed to proinflammatory signals. *Proc Natl Acad Sci U S A* 2009;106(13):5282-7. <https://doi.org/10.1073/pnas.0810909106>.
- [21] Khafaei M, Rezaie E, Mohammadi A, Shahnazi Gerdehsang P, Ghavidel S, Kadkhoda S, et al. MiR-9: From function to therapeutic potential in cancer. *J Cell Physiol* 2019;234:14651-65. <https://doi.org/10.1002/jcp.28210>.
- [22] Nowek K, Wiemer EAC, Jongen-Lavrencic M. The versatile nature of miR-9/9 in human cancer. *Oncotarget* 2018;9:20838-54. <https://doi.org/10.18632/oncotarget.24889>.
- [23] Gao S, Wang J, Tian S, Luo J. MiR9 depletion suppresses the proliferation of osteosarcoma cells by targeting p16. *Int J Oncol* 2019;54(6):1921-32. <https://doi.org/10.3892/ijo.2019.4783>.
- [24] Liu W, Liu C, Yin B, Peng XZ. Functions of miR-9 and miR-9 during aging in SAMP8 mice and their possible mechanisms. *Zhongguo Yi Xue Ke Xue Yuan Xue Bao* 2015;37(3):253-8. <https://doi.org/10.3881/j.issn.1000-503X.2015.03.001>.
- [25] Vinci S, Gelmini S, Mancini I, Malentacchi F, Pazzagli M, Beltrami C, et al. Genetic and epigenetic factors in regulation of microRNA in colorectal cancers. *Methods* 2013;59:138-46. <https://doi.org/10.1016/j.ymeth.2012.09.002>.
- [26] Ma L, Young J, Prabhala H, Pan E, Mestdagh P, Muth D, et al. MiR-9, a MYC/MYCN-activated microRNA, regulates E-cadherin and cancer metastasis. *Nat Cell Biol* 2010;12(3):247-56. <https://doi.org/10.1038/ncb2024>.
- [27] Li X, He L, Yue Q, Lu J, Kang N, Xu X, et al. MiR-9-5p promotes MSC migration by activating  $\beta$ -catenin signaling pathway. *Am J Physiol Cell Physiol* 2017;313:C80-93. <https://doi.org/10.1152/ajpcell.00232.2016>.
- [28] Laissue P. The forkhead-box family of transcription factors: Key molecular players in colorectal cancer pathogenesis. *Mol Cancer* 2019;18(1):5. <https://doi.org/10.1186/s12943-019-0938-x>.

## Related articles published in BJBMS

1. [Cisplatin inhibits the proliferation of Saos-2 osteosarcoma cells via the miR-376c/TGFA pathway](#)  
Yuan Wang et al., BJBMS, 2020
2. [EP1 receptor is involved in prostaglandin E2-induced osteosarcoma growth](#)  
Jing-cai Niu et al., BJBMS, 2019



SUPPLEMENTAL DATA

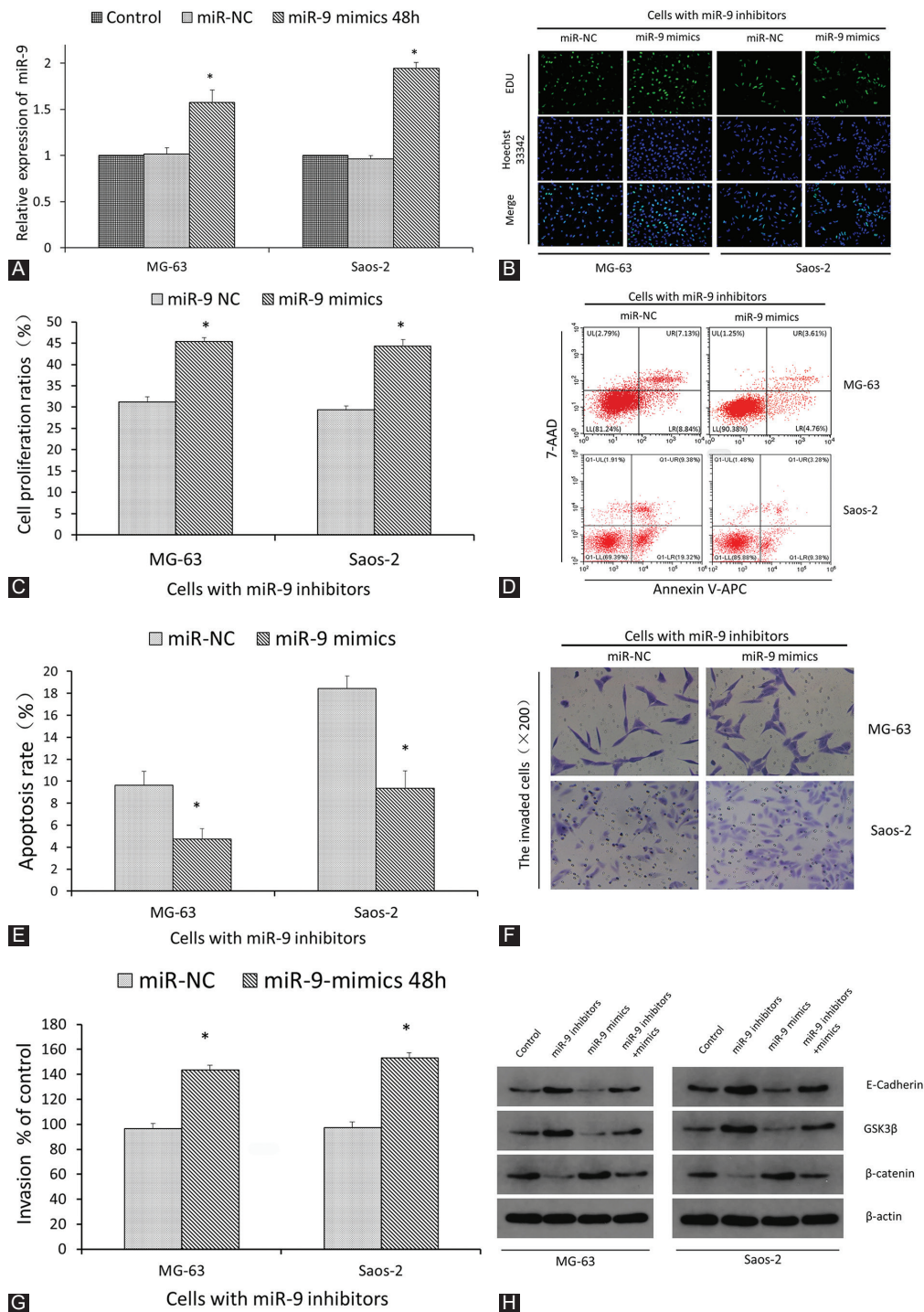


**FIGURE S1.** Effect of miR-9 mimic treatment on cell proliferation, apoptosis, and invasion ability of osteosarcoma (OS) cells. (A) miR-9 mimics significantly increased the expression of miR-9 in MG-63 and Saos-2 OS cells as determined by quantitative reverse transcription PCR (qRT-PCR); (B and C) miR-9 mimics increased the cell proliferation as determined by fluorescent-based kit. Panel B shows the representative microscopic pictures and panel C shows the quantitation of cell proliferation of OS cells; (D and E) apoptotic cells, PE (+) and 7-AAD (-), were analyzed using flow cytometry in OS cells. Apoptosis significantly decreased with the use of miR-9 mimics in OS cell lines. Panel D shows the representative flow cytometry dot-plots and panel E shows the quantitation of the same results. (F) Representative pictures of the invaded OS cells under the membrane, observed under a microscope. Scale bar = 100 mm. (G) Invasion was quantified by counting the number of MG-63 and Saos-2 cells that invaded into the inner membrane. (H) Western blots are shown for a minimum of three experiments.  $\beta$ -actin was used as the loading control. Data are presented as averages of triplicate measurements with error bars representing standard deviations \* $p < 0.05$ . GSK3 $\beta$ : Glycogen synthase kinase 3 beta.